BIOCHEMISTRY
including biophysical chemistry & molecular biology

Article

pubs.acs.org/biochemistry

Different Oligomeric Properties and Stability of Highly Homologous A1 and Proto-Oncogenic A2 Variants of Mammalian Translation Elongation Factor eEF1

Alexander A. Timchenko,[*,†] Oleksandra V. Novosylna,[‡] Eugenij A. Prituzhalov,[§] Hiroshi Kihara,[∥,⊥] Anna V. El'skaya,[‡] Boris S. Negrutskii,[‡] and Igor N. Serdyuk[†,▽]

[†]Institute of Protein Research, RAS, Pushchino 142290, Russia

[‡]State Key Laboratory of Molecular and Cellular Biology, Institute of Molecular Biology and Genetics, NAS of Ukraine, Kiev 03680, Ukraine

[§]Tula State University, Tula 300600, Russia

[∥]Department of Physics, Kansai Medical University, Hirakata, Osaka 573-1136, Japan

Supporting Information

ABSTRACT: Translation elongation factor 1A (eEF1A) directs aminoacyl-tRNA to the A site of 80S ribosomes. In addition, more than 97% homologous variants of eEF1A, A1 and A2, whose expression in different tissues is mutually exclusive, may fulfill a number of independent moonlighting functions in the cell; for instance, the unusual appearance of A2 in an A1-expressing tissue was recently linked to the induction of carcinogenesis. The structural background explaining the different functional performance of the highly homologous proteins is unclear. Here, the main difference in the structural properties of these proteins was revealed to be the improved ability of A1 to self-associate, as demonstrated by synchrotron small-angle X-ray scattering (SAXS) and analytical ultracentrifugation. Besides, the SAXS measurements at different urea concentrations revealed the low resistance of the A1 protein to urea. Titration of the proteins by hydrophobic dye 8-anilino-1-naphthalenesulfonate showed that the A1 isoform is more hydrophobic than A2. As the different association properties, lipophilicity, and stability of the highly similar eEF1A variants did not influence considerably their translation functions, at least *in vitro*, we suggest this difference may indicate a structural background for isoform-specific moonlighting roles.

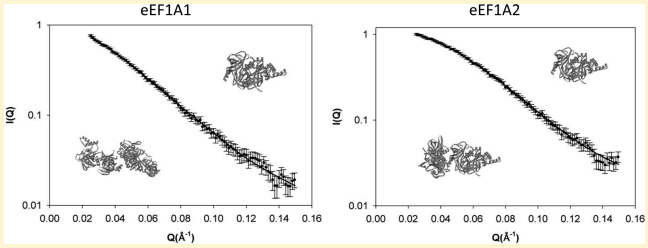

Translation elongation factor 1A (eEF1A) is a major participant in the ribosomal peptide elongation process. It forms stable complexes with GTP and aminoacyl-tRNAs of different specificities, distributing aminoacylated tRNA to the A site of 80S ribosomes. Correct codon−anticodon interaction leads to GTP hydrolysis, which finalizes the recognition process making it irreversible.[1] Leaving the ribosome, eEF1A*GDP may capture deacylated tRNA and bring it to aminoacyl-tRNA synthetase for recharging in a vectorial transfer process.[2] In higher vertebrates, there are two highly homologous isoforms of eEF1A, with scattered amino acid substitutions along the molecules ending up with more than 97% of the molecules being similar (Figure 1A). Both A1 and A2 isoforms are well-conserved (Figure 1 of the Supporting Information). For A1, a single-amino acid substitution was noticed in the mouse or bovine protein, while in A2, the only substitution was found in the mice protein. The genes for eEF1A1 (A1) and eEF1A2 (A2) are situated on different chromosomes, in humans on 6q13 and 20q13.3, respectively.[3] The A1 protein is present all over the organism except in muscles, neurons, and some specialized cells where exclusive expression of A2 is observed.[4,5] Developmentally, A1 was found to be gradually replaced by A2 in muscles during first 3 weeks of mice postnatal development. Mutational disruption of the process caused development of the wasted mouse phenotype.[6]

eEF1A fulfills many auxiliary duties in a cell, being involved in spermatogenesis,[7] cell cycle progression,[8] chaperone-mediated autophagy,[9] apoptosis,[10] and lipotoxic cell death.[11] It is also a proteolysis-related[12] and cytoskeleton-modulating[13] protein. Thus, eEF1A may serve as an important link connecting different cellular processes in the cytoplasm both physically and functionally. The distribution of eEF1A between different processes in cell remains unclear. In principle, the isoforms of eEF1A may participate in distinct cellular processes; however, one might expect a resemblance of functions performed by two highly similar proteins. Quite surprisingly, recent reports demonstrated the possibility of the exclusive involvement of a particular isoform in the complexes with both translational and nontranslational partners. For instance, as opposed to the case for A1, it was not

Received: March 28, 2013
Revised: June 17, 2013
Published: July 16, 2013

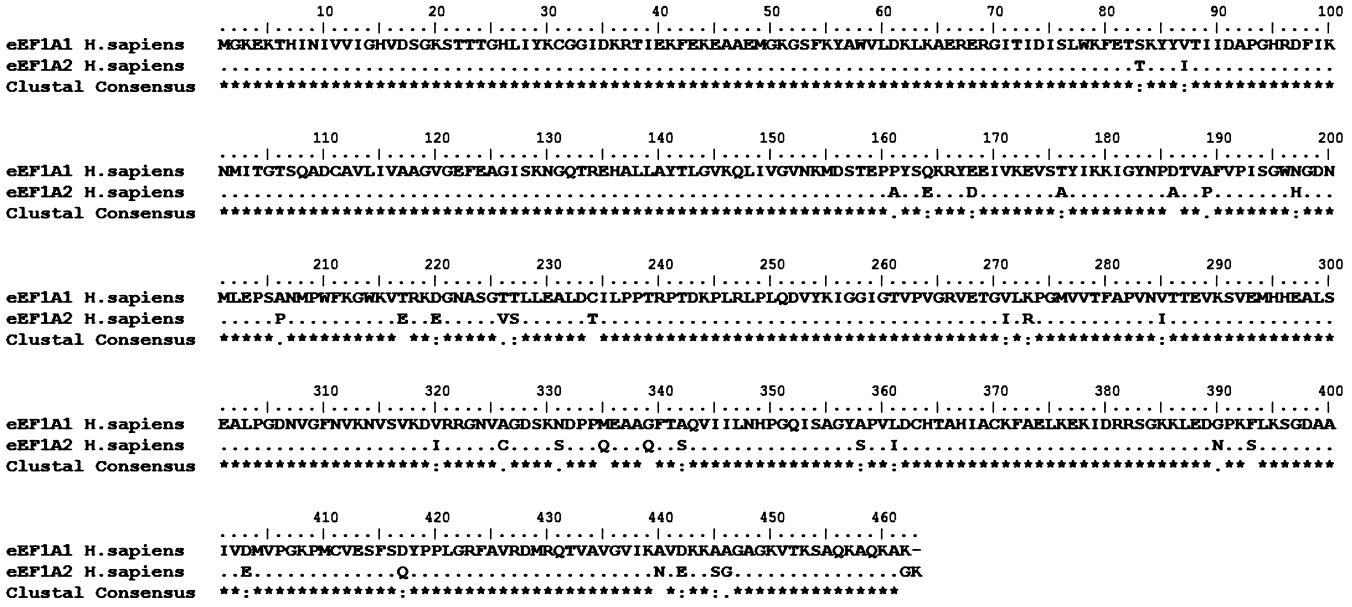

Figure 1. Sequence alignment of A1 and A2 isoforms. The substitutions are shown for A2. The alignment was generated with ClustalW and edited with BioEdit.

possible to detect the interaction of A2 with the GTP-exchanging subunits of translation elongation factor eEF1B in the yeast double-mutant system.[14] As for noncanonical roles, the A2 protein was found to possess higher potency than A1 to interact with SH2 and SH3 domains of various signaling molecules.[15] A2 rather than A1 specifically binds peroxiredoxin 1, contributing to the cell resistance against oxidative stress,[16] and also interacts with tumor supresor $p16^{INK4a}$.[17] A1 was reported to be a pro-apoptotic protein, while A2 possessed anti-apoptotic features.[18,19] Notwithstanding the fact that the A2 isoform is not normally present in tissues other than muscle and neuronal tissue, its highly elevated level of expression was detected in a number of human carcinomas in different locations,[3,20,21] demonstrating in some cases pronounced oncogenic potential.[20,22] The nature of the putative oncogeneity of the A2 isoform is not yet fully understood. Apparently, it is not related to gene amplification, mutation in coding sequence, or changes in gene methylation,[23] indicating that cancer-related properties could be inherent to the protein molecule per se.

One may assume that the functional peculiarity of an isoform is provided by its different protein- and/or RNA-interacting abilities; however, the structural background for that is unknown. Some hints about the possible structural diversity of the isoforms came from microcalorimetric measurements in which A1 and A2 were characterized by the different heat absorption values.[24] Also, the more extended shape of A1 as compared with that of bacterial analogue EF-Tu was predicted on the basis of neutron scattering studies.[25] The conformation of A2 was not investigated at that time. Molecular dynamics studies revealed only subtle difference in the dynamics of A1 and A2 proteins.[26] In another study, comparison of the A1 and A2 models did not demonstrate a noticeable difference either.[27]

Here, as a result of fluorescence titration experiments, A1 was characterized by a 10-fold greater coefficient of hydrophobicity than A2. Small-angle X-ray scattering (SAXS) showed the A1 protein was prone to urea-induced denaturation, losing its regular structure at 2−3 M urea, and A2 has undergone such a loss at 3−4 M urea. However, SAXS did not reveal a profound difference in the molecular shape of the A1 and A2 proteins. Instead, A1 was observed to possess significant ability to self-associate, mostly as dimers. Different self-association properties, stability, and hydrophobicity of the highly similar isoforms of eEF1A are assumed to serve as a structural background for the isoform-specific interactions with cellular proteins, which are not directly related to ribosomal translation.

EXPERIMENTAL PROCEDURES

Isolation of Biological Macromolecules. The A1 and A2 proteins were purified from rabbit liver and muscles, respectively, as described previously.[15] Total tRNA was isolated from rabbit liver and yeast according to the conventional procedure.[28] 40S and 60S ribosomal subunits were obtained from rabbit liver as described previously.[29] Recombinant human $tRNA_3^{Lys}$ was kindly supplied by M. Mirande; phenylalanyl-tRNA synthetase was a gift from T. Lukash, and elongation factor eEF2 was contributed by T. Budkevich.

Small-Angle X-ray Scattering. The SAXS measurements were performed in the small-angle chamber BL-15A instrument at Photon Factory (Tsukuba, Japan). The protein solution in the thermostated cell with mica windows was irradiated by X-rays with a wavelength of 1.503 Å at room temperature. To prevent X-ray irradiation damage of the proteins, several short scans were stored and analyzed. The distance between the sample and source was 2.35 m. The range of detectable scattering vectors (Q) was 0.011−0.15 $Å^{-1}$ ($Q = 4\pi \sin \theta/\lambda$, where λ is the wavelength of X-rays and 2θ the scattering angle). The data registered by the two-dimensional CCD X-ray detector[30] were corrected for image distortion, nonlinear response, and contrast according to the method described in ref 31. The SAXS patterns were assessed by the homemade SAXTIM program (unpublished). To determine the molecular masses of the proteins from the initial ordinate of the scattering curve, the measurement of reference protein bovine serum albumin (BSA) was performed. The eEF1A isoforms (concentration range of 2−4 mg/mL) were measured in buffer containing 30 mM Tris-HCl (pH 7.5), 1 mM $MgCl_2$, 10 mM KCl, 6 mM β-mercaptoethanol, 20 μM GDP, and 20% glycerol.

dx.doi.org/10.1021/bi400400r | Biochemistry 2013, 52, 5345−5353

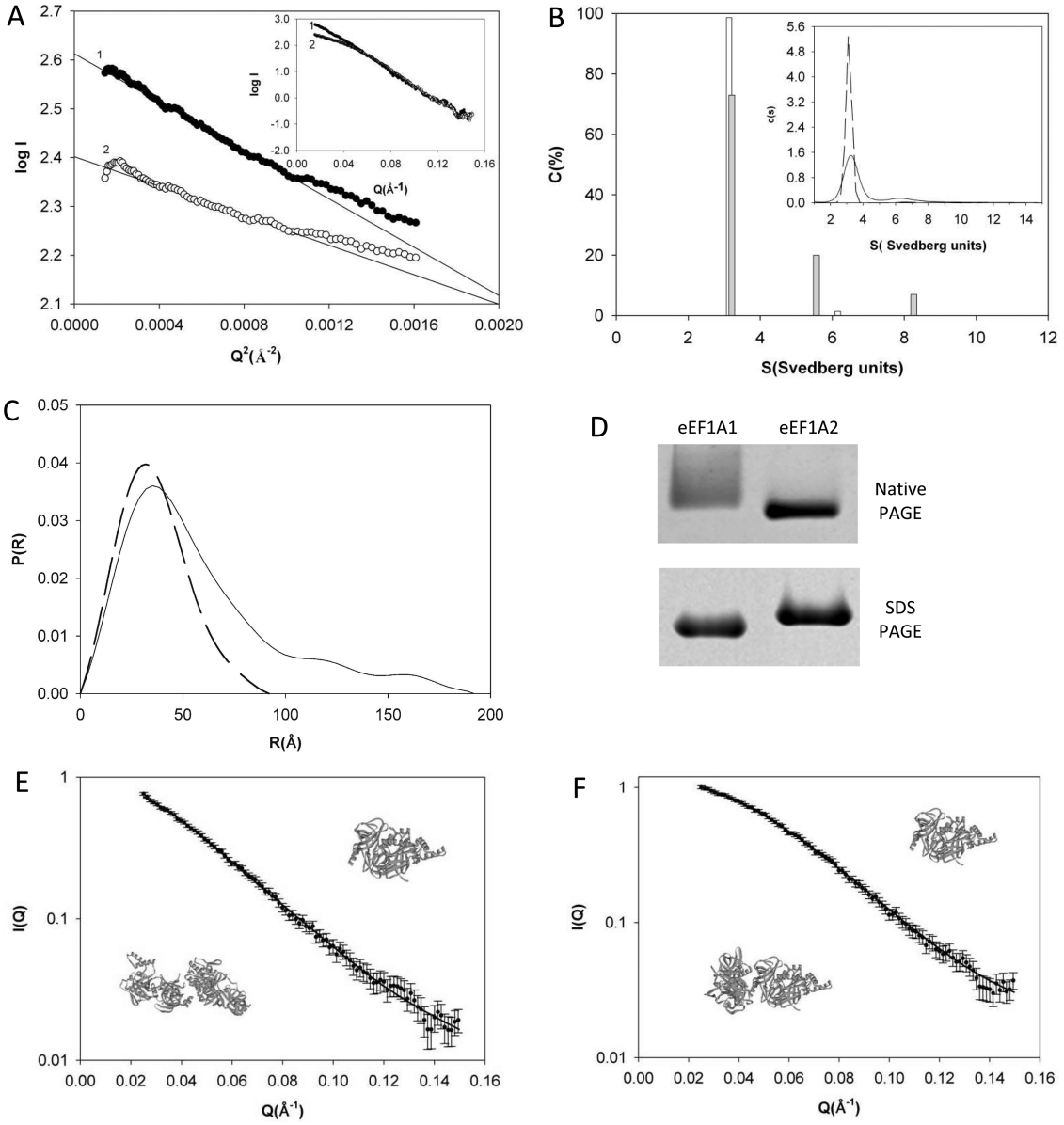

Figure 2. A1 and A2 proteins show different oligomeric properties. (A) Guinier plots (log I vs Q^2) for determining the average dimensions of the A1 (1) and A2 (2) particles from the SAXS data. The inset shows SAXS patterns for A1 (1) and A2 (2). Concentrations of A1 and A2 were 2.6 and 3.4 mg/mL, respectively. (B) Discrete sedimentation coefficient distribution $c(s)$ for A1 (filled columns, rmsd of 0.0072) and A2 (empty columns, rmsd of 0.0074). The values of sedimentation coefficients were 3.3 and 3.18 S, respectively. The inset shows a continuous sedimentation coefficient distribution $c(s)$ for A1 (solid line, rmsd of 0.0156) and A2 (dashed line, rmsd of 0.0131). (C) Pair distribution function plot for the A1 (solid line) and A2 (dotted line) particles from the SAXS data. (D) Electrophoretic behavior of the A1 and A2 proteins in the gels run under denaturing and nondenaturing conditions. For native polyacrylamide gel electrophoresis, 2 μg of A1 or A2 was applied to a 5% polyacrylamide gel [5% glycerol and 50 mM Tris-borate (pH 7.4)]. For sodium dodecyl sulfate−polyacrylamide gel electrophoresis, A1 and A2 (3 μg each) were boiled in the presence of sodium dodecyl sulfate and 2-mercaptoethanol, applied to a 10% polyacrylamide gel, and run in 25 mM Tris, 192 mM glycine, and 0.1% sodium dodecyl sulfate (pH 8.3). Both procedures were performed at room temperature for 2 h. (E) Experimental SAXS patterns of A1 (points) and those calculated from the monomer−dimer system (line). The inset shows the structure of the monomer and dimer. (F) Experimental SAXS patterns of A2 (points) and those calculated from the monomer−dimer system (line). The inset shows the structure of the monomer and dimer.

SAXS patterns for molecular structures with known atomic coordinates were estimated with CRYSOL.[32] Coordinates of yeast eEF1A [Protein Data Bank (PDB) entry 1F60] were used. The dimer structures were constructed via rotation of the monomers by the corresponding Euler angles, permitting the monomers to contact each other; 729 dimer structures were analyzed. The fitting of calculated SAXS patterns to the experimental ones was performed by minimization of χ^2:

$$\chi^2 = \frac{1}{N-1}\sum_j \left[\frac{I_{exp}(Q_j) - cI_{calcd}(Q_j)}{\sigma(Q_j)}\right]^2$$

where N is the number of experimental points, c is a scaling factor, which is chosen by minimizing χ^2, $I_{exp}(Q_j)$ and $I_{calcd}(Q_j)$ are experimental and calculated intensities, respectively, and $\sigma(Q_j)$ is the experimental error at the momentum transfer Q_j.

Sedimentation Velocity Analysis. The experiments were conducted in a Beckman Optima XL-I centrifuge. Samples were

dx.doi.org/10.1021/bi400400r | *Biochemistry* 2013, 52, 5345−5353

spun for 40 min at 50000 rpm and 20 °C, with 8 min time intervals and 0.003 cm resolution with no delay between scans. Sedimentation was performed in two-sector cells using the An60 rotor. The protein concentration was 1−1.5 mg/mL. The sedimentation data were treated with SEDFIT.[33] The experimental s values were corrected for the standard state of water at 20 °C[34] (solvent density of 1.0561 g/cm^3 and viscosity of 1.984 cP). Sedimentation coefficients of the proteins with known tertiary structure were calculated with "HydroPro".[35] The partial specific volume of the proteins derived from amino acid composition[36] was 0.743 cm^3/g.

ANS Fluorescence. The fluorescent probe 8-anilino-1-naphthalenesulfonate (ANS) was used for determination of the surface hydrophobic properties of eEF1A. Free ANS fluoresces very weakly in water, but the quantum yield of fluorescence sharply increases upon interaction of ANS with the protein hydrophobic sites. ANS (0, 2, 4, 8, 16, 32, and 64 μM) was mixed with 6 μM eEF1A1 or eEF1A2 in 30 mM Tris-HCl (pH 7.5) containing 20% glycerol, 1 mM $MgCl_2$, and 6 mM β-mercaptoethanol. Inversely, eEF1A (0−20 μM) was added to 4 μM ANS. Fluorescence spectra were recorded with a Cary Eclipse (Varain) fluorescence spectrophotometer at 25 °C using an excitation wavelength of 360 nm and scanning the emission from 400 to 600 nm with a path length of 1 cm.

The relative fluorescence (F_R) was calculated according to the equation[37] $F_R = (F - F_0)/F_0$, where F is the fluorescence intensity of ANS bound to the protein and F_0 is the fluorescence intensity of ANS in the buffer. F_R was plotted versus eEF1A or ANS concentration. The index of the protein surface hydrophobicity was obtained by measuring the initial slope of the fluorescence intensity versus protein concentration curve[38] using GraphPad Prism 5.

Functional Tests. Nucleotide exchange properties of A1 and A2 were studied as described in ref 4. The polypeptide chain elongation activities of A1 and A2 were compared in the poly(U) translation system assembled from individual components.[39] The ability of A1 and A2 to form the complexes with nonacylated $tRNA_3^{Lys}$ was examined in the band-shift assay. tRNA was labeled with [α-^{32}P]ATP as described previously.[40] Incubation of [^{32}P]tRNA and different amounts of the eEF1A isoforms was conducted in 10 μL of buffer containing 20 mM Tris-HCl (pH 7.5), 50 mM KCl, 5 mM $MgCl_2$, 2 mM DTT, 200 μM GDP, and 10% glycerol for 15 min at 37 °C. The incubation mixture was applied to a 5% polyacrylamide gel, prepared in 12 mM Tris-borate buffer (pH 7.5) containing 0.5 mM EDTA and 5% glycerol. Electrophoresis was conducted for 2 h at 4 °C and 100 V. The gel was dried out on the paper sheet and radioautographed for 18 h at 4 °C.

RESULTS

Evaluation of the Dimensions and Molecular Masses of A1 and A2 from the SAXS Data. We took advantage of the mutually exclusive expression of the eEF1A isoforms in rabbit tissues to isolate non-cross-contaminated preparations of A1 from liver and A2 from muscles. Thus, the proteins maintained natively folded conformations and post-translational modifications. The absence of high-molecular weight aggregates in the preparations of both isoforms was confirmed by laser light scattering (data not shown).

The SAXS curves of the A1 and A2 proteins were plotted in Guinier coordinates to evaluate the average dimensions of scattering particles and their molecular masses (Figure 2A and Table 1). Comparison of the experimentally determined and amino acid composition-based molecular masses revealed the essential heterogeneity of the A1 sample, while A2 retained a minor amount of associates in solution. The latter observation was supported by sedimentation velocity analysis (Figure 2B) where the presence of associates in the A1 preparation was also detected. A continuous $c(s)$ distribution (Figure 2B, inset) with a root-mean-square deviation (rmsd) of 0.0156 clearly demonstrates the heterogeneity of the A1 sample over a restricted range of sedimentation values. For proteins with a discrete distribution of molecular masses (monomer, dimer, etc.), the use of the "noninteracting discrete species" option of SEDFIT is recommended. The best fit of sedimentation data for A1 was obtained using the three-component distribution (monomer, dimer, and trimer) with an rmsd of 0.0072. The obtained 5.6 S value for the dimer fraction corresponds to the compact dimer of the 50 kDa globular protein. It is important to note that dimerization of eEF1A was detected recently in the *Tetrahymena*,[41,42] mouse embryo lysate,[43] and mammalian[44,45] cell lines.

Table 1. Comparison of the Experimental (exp) and Theoretical (calcd) Values of Molecular Mass (M) and Radius of Gyration (R_g) of Different Elongation Factors[a]

protein	M (kDa) (calcd)	M (kDa) (exp)	R_g (Å) (calcd)	R_g (Å) (Guinier)	R_g (Å) (Kratky)
eEF1A (yeast)	48.1	–	25		
eEF1A1 (rabbit liver)	50.2	82 ± 4		41.4 ± 1.0	36.9 ± 2.0
eEF1A2 (rabbit muscle)	50.6	58 ± 4		29.1 ± 1.0	27.9 ± 2.0

[a]Experimental values were calculated from the Kratky and Guinier plots. The scattering from yeast eEF1A was calculated using the published PDB structure of this protein. To avoid the contribution of macromolecular associates (trimers and higher-order associates), the modeled curves were fit to the experimental ones in the range $Q > 1/R_g$, where R_g is the monomer radius of gyration. The Q values were from 0.025 to 0.15 Å^{-1}.

Experimentally determined R_g values listed in Table 1 for A1 (41.4 ± 1.0 Å) and A2 (29.1 ± 1.0 Å) exceeded that for the crystal structure of yeast EF1A (25 Å), mostly because of the heterogeneity of the samples that was especially evident in the case of A1. The R_g value was determined also from the position of the maximum on the Kratky plot.[46] In this case, the R_g value was estimated at the momentum transfer value $Q > 1/R_g$. Under these conditions, the input of the oligomers to the SAXS pattern is essentially diminished in comparison with the contribution of the monomer and dimer. The same tendency of the R_g value of A1 to be essentially higher than that for A2 was observed (Table 1). A clearer pattern of the sample heterogeneity is seen from the pair distribution function $P(r)$ calculated by GNOM.[47] $P(r)$ for A1 has two shoulders corresponding most likely to the dimer and trimer (Figure 2C), in accordance with sedimentation data (Figure 2B), while $P(r)$ for A2 was typical for a globular protein (Figure 2C). Comparison of the SAXS patterns for A1 and A2 (Figure 2A, inset) indicates their difference is pronounced in the small-angle region where the contribution of associates is essential. These data can be interpreted as demonstrating the essential ability of A1 to self-associate as compared to A2. It is worth underlining that similar behavior of the SAXS patterns was observed for three different preparations of A1 and A2 (data not shown). As the SAXS experiments required relatively large amounts of protein, the homogeneity of the A1 and A2 samples in the physiologically relevant concentrations was examined by gel electrophoresis under nondenaturing conditions (Figure 2D). The essential heterogeneity of the A1 sample was observed, supposedly due to the dissociation of dimers in the gel during electrophoresis, contrary to the preferentially homogeneous A2

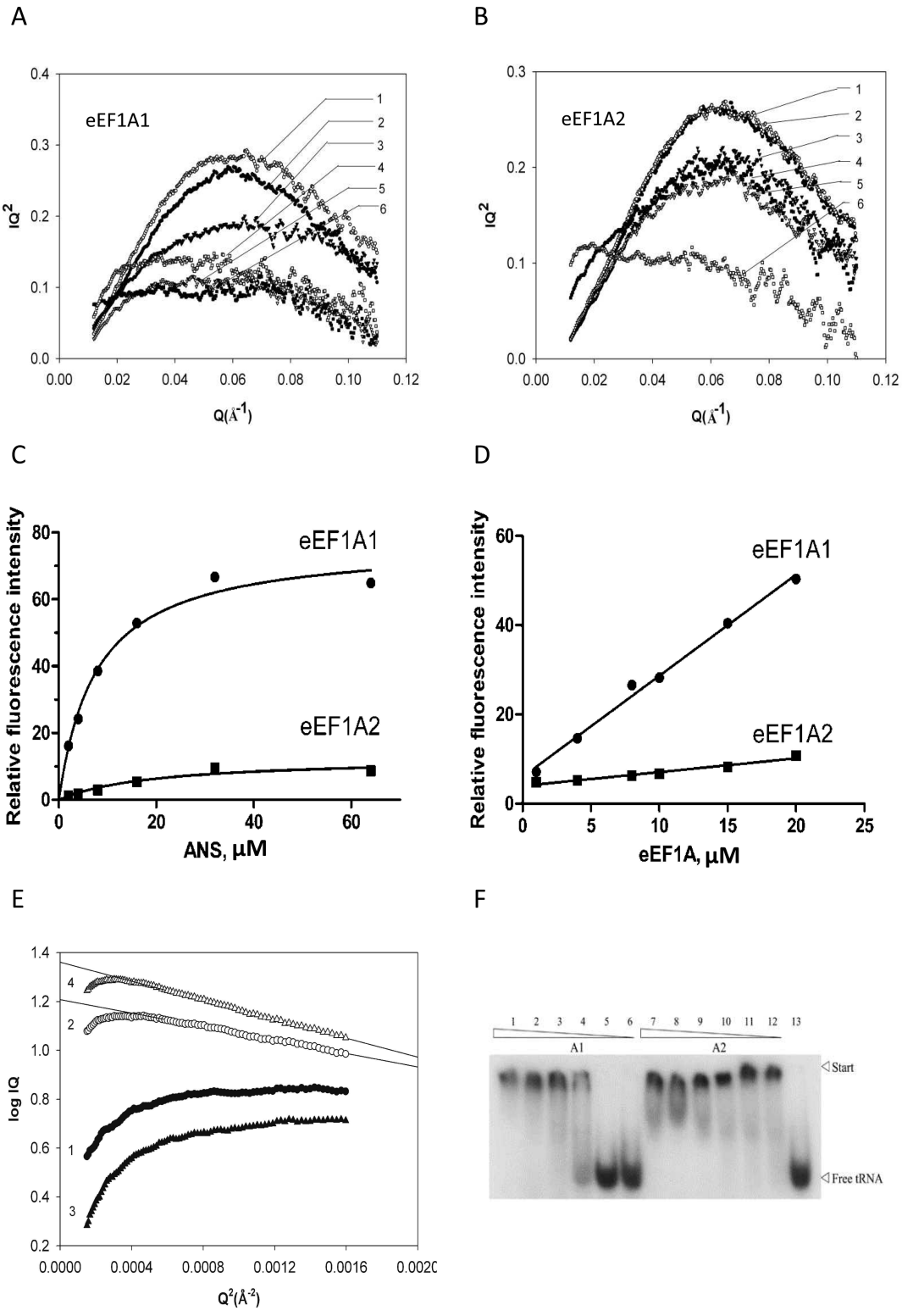

Figure 3. Difference in the molecular organization of the A1 and A2 proteins. Kratky plots (A) for A1 at different urea concentrations and (B) for A2 at different urea concentrations: (1) no addition, (2) 1 M urea, (3) 2 M urea, (4) 3 M urea, (5) 4 M urea, and (6) 5 M urea. Each third experimental point is shown. (C) Titration of 6 μM A1 or A2 with varying concentrations of ANS. (D) Change in the relative fluorescence intensity of 4 μM ANS upon addition of different concentrations of A1 or A2. (E) SAXS patterns [log(IQ) vs Q^2] for A1 (1), A1 with tRNA (2), A2 (3), and A2 with tRNA (4). (F) Titration of A1 or A2 with [^{32}P]tRNA$_3^{Lys}$ in a gel-shift experiment. tRNA was titrated with different (2, 1, 0.5, 0.25, 0.12, and 0.06 μM) concentrations of the A1 isoform (lanes 1−6) and the A2 isoform (lanes 7−12). Lane 13 contained free tRNA.

preparation. Both proteins were homogeneous in the sodium dodecyl sulfate gel (Figure 2D). Full-line gels are shown in Figure 2 of the Supporting Information.

Next, we estimated the contribution of trimers to the scattering as the presence of trimers in the protein preparation was detected by sedimentation analysis. For that, we modeled the

dx.doi.org/10.1021/bi400400r | *Biochemistry* 2013, 52, 5345−5353

compact trimer structure and calculated the SAXS pattern from the mixture of compact monomers, dimers, and trimers, keeping their ratio in accordance with the sedimentation data. The contribution of trimers to the SAXS pattern was found to be insignificant, representing 3% at 0.025 $Å^{-1}$ and rapidly decreasing at higher Q values.

The experimental scattering patterns were fit to those from the mixture of calculated SAXS patterns for the monomer and dimer by solving a system of linear equations. The algorithm of nonnegative least-squares was employed to minimize the divergence between the experimental and calculated scattering curves; 729 different structures of dimers were analyzed, and the best fit was chosen. The result of the best fit (χ^2 = 0.31) for A1 is presented in Figure 2E. In this case, the weight fraction of dimers equals 0.8. The found structure of the dimer with an R_g of 37.3 Å is represented in the inset of Figure 2E. The analogous best fit (χ^2 = 0.29) for A2 is presented in Figure 2F. In this case, the weight fraction of dimers is 0.28. The found structure of the dimer with an R_g of 33.7 Å is represented in the inset of Figure 2F. The values of the dimer weight fractions correlated with the evaluations of molecular masses from Guinier plot (see Table 1).

Thus, the A1 and A2 isoforms of translation elongation factor 1A, which are more than 97% similar, demonstrate, nevertheless, quite different self-association properties. Contrary to A2, A1 has an essential tendency to associate, mostly as dimers.

Treatment of the A1 and A2 Isoforms with Urea. The difference in the R_g values of the A1 and A2 dimers hints at the possibility of the nonequality of the molecular organization of the monomers resulting in their different stabilities as shown recently by calorimetric tests.[24] To examine the point further, the SAXS measurements of A1 and A2 were conducted in the presence of increasing concentrations of urea. Urea is the most appropriate SAXS measurement reagent because it possesses electron density and X-rays absorption properties similar to those of water. Evidence of the compactness of a particle is the presence of a distinct maximum in the Kratky graph.[47] Indeed, the response of the isoform structures to the increasing urea concentrations was found to be different. According to this criterion, the A1 protein compactness was lost at 2−3 M urea (Figure 3A) while the A2 tertiary structure was "melted" at 3−4 M urea (Figure 3B), demonstrating the increased resistance of A2 to the denaturing agent compared to that of A1.

Different Surface Hydrophobicities of the A1 and A2 Isoforms. Hydrophobic forces are believed to be among the major determinants of protein aggregation,[48] so the increased susceptibility of the A1 protein to aggregation hints at its augmented lipophilicity. As the presence of additional hydrophobic regions in an isoform may be responsible for its improved ability to interact with specific cellular ligands, the comparative hydrophobicity of the isoforms was investigated by titration with fluorescent agent ANS.[37,38] Figure 3C shows that the A1 protein, contrary to A2, efficiently binds ANS, demonstrating the more hydrophobic character of its surface. The level of surface hydrophobicity was estimated according to ref 38 as the initial slope of the fluorescence intensity versus protein concentration (Figure 3D). The surface hydrophobicity coefficient was calculated to be 2.26 for A1 and 0.27 for A2. It should be noted, however, that by taking into account the hydrophobicity scale for different cellular proteins[37] we found neither A1 nor A2 is an essentially hydrophobic protein, although the difference in the hydrophobic coefficients for the A1 and A2 proteins is important because it indicates the presence in A1 of additional local hydrophobic region(s), which could be significant for an increased level of self-association of A1 and for its interaction with different protein partners.

Elongated Shape of the Complexes of A1 and A2 with tRNA. A1 is known to form a rather stable complex with deacylated tRNA.[49,50] To compare the tRNA binding abilities of A1 and A2 and the shapes of their complexes with tRNA, the corresponding scattering patterns were examined with an excess of protein (2:1 protein:tRNA molar ratio). The data are presented in the coordinates log(IQ) versus Q^2, which can be used to characterize the elongated molecules and permit calculation of the R_g of the cross section (R_c).[51] The linear dependence was observed for the A1*GDP*tRNA and A2*GDP*tRNA complexes rather than for the individual A1 and A2 proteins (Figure 3E). We interpret this result as favoring an elongated shape of A1/A2 complexes with tRNA in solution. The evaluation of R_c from the slope gives values of 25 and 30 Å for A1 and A2, respectively. The corresponding values of R_g for the A1 and A2 complexes with tRNA were 62.4 and 65.4 Å, respectively. In the case of a uniform approximation, one can evaluate the length (L) of particles according to the relationship $L^2 = 12(R_g^2 - R_c^2)$.[51] L was ∼200 Å for both complexes. The evaluation of the molecular mass from $I(0)$ showed that under these conditions the elongated complex may comprise three to four A1/A2 molecules per tRNA.

tRNA binding properties of A1*GDP and A2*GDP complexes at physiologically relevant concentrations were assessed by their ability to interact with deacylated tRNA in a gel-shift assay. The ternary complexes involving $tRNA_3^{Lys}$ were formed by both isoforms, the A2-containing complex being somewhat more stable (Figure 3F). A similar trend was found for tRNAs of nine amino acid specificities (data not shown).

Functional Tests. Various *in vitro* tests of A1 and A2 were performed to reveal the possible impact of the enhanced aggregation state of A1 on its translation functions. Titration of [^{3}H]GDP or [^{3}H]GTP with increasing amounts of A1*GDP or A2*GDP indicated a similar affinity of A1 for GDP and GTP while A2 preferentially bound GDP (Figure 3A,B of the Supporting Information), in agreement with earlier findings.[4] The A1 and A2 isoforms were shown to possess comparable translation potentials *in vitro* as judged from their ability to stimulate translation of poly(U) in the cell-free system assembled from individual components (Figure 3C of the Supporting Information).

DISCUSSION

Here, the A1 and A2 isoforms of mammalian translation elongation factor eEF1A have been shown to exhibit pronounced differences in their self-association properties, regardless of the same domain organization and a very high degree of sequence homology. Such dissimilarity may result from the different structural organization of A1 and A2 reflected by the unequal resistance of the isoforms to urea (Figure 3C,D). This conclusion is also supported by the published results of scanning microcalorimetry demonstrating quite different values of the heat absorption of A1 and A2 during denaturation; i.e., in the case of A1, the specific enthalpy value ΔH_{cal} was nearly 2 times lower than that of A2.[24]

An intriguing question is which structural elements may provide a noticeable difference in the molecular organization and association properties of more than 97% similar isoforms. We may consider at least two explanations for that: (i) local conformational changes resulting from the differences in primary structures or (ii) different post-translational modifications. A synergic

effect cannot be excluded either because local conformational changes in eEF1A may be caused by specific post-translational modifications.[52]

The enhanced hydrophobic properties of A1 (Figure 3C,3D) may contribute to its enhanced ability to associate; however, previous structural modeling and molecular dynamic studies were not able to reveal essential structural difference between the isoforms.[26,27] However, in this case, the template for modeling was the crystal structure of yeast eEF1A bound to nucleotide exchange factor.[53] In this complex, eEF1A is trapped on its way from the GDP-bound form to the GTP-bound form; subsequently, this intermediate state can be different from the stable eEF1A*GDP conformation investigated here.

As there are known examples of how the spatial structure of a protein can be crucially changed upon substitution of very few amino acids,[54,55] that could be the case for the eEF1A isoforms. The high level of conservation of the eEF1A sequences suggests that almost every surface of the protein molecule is involved in core protein−protein interaction, so as little as 3% nonidentity of the sequences may still provide a basis for the isoform-specific protein−protein interplay as observed for the interaction of A1 or A2 with calmodulin,[26] tumor supresor $p16^{INK4a}$,[17] or peroxiredoxin 1.[16]

The effect of different levels of post-translational modification in the isoforms should be also considered. Several lysine residues are dimethylated or trimethylated in eEF1A.[56] There are indications that the number of methylated lysines and the level of their modifications in the isoforms may be different,[4,56] which may contribute to the distinct hydrophobicity of the protein surface. The effect of phosphorylation may be important as well. For instance, the ability of 85% identical histone deacetylase 1 and 2 to form homodimers was recently reported to be linked to their phosphorylation status.[57] As eEF1A1 and eEF1A2 isoforms may possess different phosphorylation sites,[52] the possibility of a contribution of the phosphorylation to the enhanced ability of eEF1A1 to self-associate cannot be excluded. The effect of phosphorylation may be indirect, i.e., influencing the local conformation of the molecule.

The translational role of dimers of bacterial EF-Tu*GTP dimers was suggested some time ago;[58] however, this concept was not developed further. It is unclear yet whether the dimers function in eukaryotic translation. Thus, the importance of the different self-association properties of the eEF1A isoforms for local protein synthesis awaits further examination. Still, that may have independent significance for the moonlighting functions of the isoforms. Usually, the expression of A1 and A2 is mutually exclusive and tissue-specific. Their long-term concurrent expression in the same tissue was possible only under an abnormal condition for that particular tissue situation, such as tumorigenesis (unusual appearance of A2)[3,20] or muscle denervation/regeneration (bonus appearance of A1).[59,60] Opposite functions of A1 and A2 in apoptosis have been described previously.[18,19] There were also reports of the appearance of A1 in the A2-expressing neurons where A1 was involved in the long-term potentiation and long-term depression processes.[61−63] Thus, the different structural organization of the isoforms may be a prerequisite for the attainment of some novel protein−protein interactions causing unusual and not always favorable (as in the case of eEF1A2-driven oncogenesis) consequences for a given type of cells.

Importantly, contrary to some cellular proteins, the different oligomeric state does not influence the biological activity of the isoforms in translation. The formation and importance of A1/A2 heterodimers remains to be confirmed by physical methods, though recent pull-down assays seem to elucidate such an option.[43] The distinct ability of the eEF1A isoforms to associate may have biologically important consequences; for instance, dimerization of eEF1A was suggested to have an impact on phosphorylation of its Ser21 residues by Raf kinases, with a subsequent effect on cell proliferation and apoptosis.[44]

We present here a snapshot of the current understanding of the physical properties of A1 and A2. The 97% identical isoforms of eEF1A possess differences in spatial organization, including the more pronounced ability of eEF1A1 to self-associate. A distinct hydrophobicity level may be among the reasons providing such a difference. Further investigations are needed to determine the exact reason for the enhanced oligomerization capacity of eEF1A1, regulation of the dimer−monomer equilibrium, and ability to form heterodimers with eEF1A2 *in cellulo*. The amino acid background for the specific self-association properties and molecular organization of the eEF1A isoforms will be revealed in the future large-scale mutagenesis studies.

■ ASSOCIATED CONTENT

Supporting Information

Figures S1−S3. This material is available free of charge via the Internet at http://pubs.acs.org.

■ AUTHOR INFORMATION

Corresponding Author

*Institute of Protein Research, RAS, Pushchino, Moscow Region 142290, Russia. E-mail: atim@vega.protres.ru. Telephone: 7(495)5140218. Fax: 7(4967)318435.

Present Address

⊥H.K.: SR Center, Ritsumeikan University, 1-1-1 Noji-Higashi, Kusatsu 525-8577, Japan.

Author Contributions

A.A.T. and O.V.N. contributed equally to this work.

Funding

The work was approved by the Photon Factory (Proposal 2007G645). The support of the Collaborative grant programs of NASU with RAN and CNRS is acknowledged.

Notes

The authors declare no competing financial interest.

▽Deceased March 23, 2012.

■ ACKNOWLEDGMENTS

We appreciate the participation of P. V. Futernyk and A. P. Pogribna in the functional characterization of the isoforms as well as the help of D. O. Vlasenko and P. V. Molodchyk with computer modeling. We thank to T. V. Budkevich for the critical reading of the manuscript.

■ ABBREVIATIONS

eEF1A, eukaryotic translation elongation factor 1A; A1, isoform 1 of eEF1A; A2, isoform 2 of eEF1A; ANS, 8-anilino-1-naphthalenesulfonate; SAXS, small-angle X-ray scattering; BSA, bovine serum albumin.

■ REFERENCES

(1) Mateyak, M. K., and Kinzy, T. G. (2010) eEF1A: Thinking outside the ribosome. *J. Biol. Chem. 285*, 21209−21213.

(2) Negrutskii, B. S., and El'skaya, A. V. (1998) Eukaryotic translation elongation factor 1α: Structure, expression, functions, and possible role

in aminoacyl-tRNA channeling. *Prog. Nucleic Acid Res. Mol. Biol. 60*, 47−78.
(3) Tomlinson, V. A., Newbery, H. J., Wray, N. R., Jackson, J., Larionov, A., Miller, W. R., Dixon, J. M., and Abbott, C. M. (2005) Translation elongation factor eEF1A2 is a potential oncoprotein that is overexpressed in two-thirds of breast tumours. *BMC Cancer 5*, 113.
(4) Kahns, S., Lund, A., Kristensen, P., Knudsen, C. R., Clark, B. F., Cavallius, J., and Merrick, W. C. (1998) The elongation factor 1 A-2 isoform from rabbit: Cloning of the cDNA and characterization of the protein. *Nucleic Acids Res. 26*, 1884−1890.
(5) Newbery, H. J., Loh, D. H., O'Donoghue, J. E., Tomlinson, V. A., Chau, Y. Y., Boyd, J. A., Bergmann, J. H., Brownstein, D., and Abbott, C. M. (2007) Translation elongation factor eEF1A2 is essential for post-weaning survival in mice. *J. Biol. Chem. 282*, 28951−28959.
(6) Chambers, D. M., Peters, J., and Abbott, C. M. (1998) The lethal mutation of the mouse wasted (wst) is a deletion that abolishes expression of a tissue-specific isoform of translation elongation factor 1α, encoded by the Eef1a2 gene. *Proc. Natl. Acad. Sci. U.S.A. 95*, 4463−4468.
(7) Tash, J. S., Chakrasali, R., Jakkaraj, S. R., Hughes, J., Smith, S. K., Hornbaker, K., Heckert, L. L., Ozturk, S. B., Hadden, M. K., Kinzy, T. G., Blagg, B. S., and Georg, G. I. (2008) A novel potent indazole carboxylic acid derivative blocks spermatogenesis and is contraceptive in rats after a single oral dose. *Biol. Reprod. 78*, 1139−1152.
(8) Mishra, A. K., Gangwani, L., Davis, R. J., and Lambright, D. G. (2007) Structural insights into the interaction of the evolutionarily conserved ZPR1 domain tandem with eukaryotic EF1A, receptors, and SMN complexes. *Proc. Natl. Acad. Sci. U.S.A. 104*, 13930−13935.
(9) Bandyopadhyay, U., Sridhar, S., Kaushik, S., Kiffin, R., and Cuervo, A. M. (2010) Identification of regulators of chaperone-mediated autophagy. *Mol. Cell 39*, 535−547.
(10) Lamberti, A., Caraglia, M., Longo, O., Marra, M., Abbruzzese, A., and Arcari, P. (2004) The translation elongation factor 1A in tumorigenesis, signal transduction and apoptosis: Review article. *Amino Acids 26*, 443−448.
(11) Borradaile, N. M., Buhman, K. K., Listenberger, L. L., Magee, C. J., Morimoto, E. T., Ory, D. S., and Schaffer, J. E. (2006) A critical role for eukaryotic elongation factor 1A-1 in lipotoxic cell death. *Mol. Biol. Cell 17*, 770−778.
(12) Chen, L., and Madura, K. (2005) Increased proteasome activity, ubiquitin-conjugating enzymes, and eEF1A translation factor detected in breast cancer tissue. *Cancer Res. 65*, 5599−5606.
(13) Jeganathan, S., Morrow, A., Amiri, A., and Lee, J. M. (2008) Eukaryotic elongation factor 1A2 cooperates with phosphatidylinositol-4 kinase IIIβ to stimulate production of filopodia through increased phosphatidylinositol-4,5 bisphosphate generation. *Mol. Cell. Biol. 28*, 4549−4561.
(14) Mansilla, F., Friis, I., Jadidi, M., Nielsen, K. M., Clark, B. F., and Knudsen, C. R. (2002) Mapping the human translation elongation factor eEF1H complex using the yeast two-hybrid system. *Biochem. J. 365*, 669−676.
(15) Panasyuk, G., Nemazanyy, I., Filonenko, V., Negrutskii, B., and El'skaya, A. V. (2008) A2 isoform of mammalian translation factor eEF1A displays increased tyrosine phosphorylation and ability to interact with different signalling molecules. *Int. J. Biochem. Cell Biol. 40*, 63−71.
(16) Chang, R., and Wang, E. (2007) Mouse translation elongation factor eEF1A-2 interacts with Prdx-I to protect cells against apoptotic death induced by oxidative stress. *J. Cell. Biochem. 100*, 267−278.
(17) Lee, M. H., Choi, B. Y., Cho, Y. Y., Lee, S. Y., Huang, Z., Kundu, J. K., Kim, M. O., Kim, D. J., Bode, A. M., Surh, Y. J., and Dong, Z. (2013) Tumor suppressor p16INK4a inhibits cancer cell growth by down-regulating eEF1A2 through a direct interaction. *J. Cell Sci. 126*, 1744−1752.
(18) Borradaile, N. M., Buhman, K. K., Listenberger, L. L., Magee, C. J., Morimoto, E. T., Ory, D. S., and Schaffer, J. E. (2006) A critical role for eukaryotic elongation factor 1A-1 in lipotoxic cell death. *Mol. Biol. Cell 17*, 770−778.
(19) Li, Z., Qi, C. F., Shin, D. M., Zingone, A., Newbery, H. J., Kovalchuk, A. L., Abbott, C. M., and Morse, H. C., III (2010) Eef1a2 promotes cell growth, inhibits apoptosis and activates JAK/STAT and AKT signaling in mouse plasmacytomas. *PLoS One 5* (5), e10755.
(20) Anand, N., Murthy, S., Amann, G., Wernick, M., Porter, L. A., Cukier, I. H., Collins, C., Gray, J. W., Diebold, J., Demetrick, D. J., and Lee, J. M. (2002) Protein elongation factor EEF1A2 is a putative oncogene in ovarian cancer. *Nat. Genet. 31*, 301−305.
(21) Li, R., Wang, H., Bekele, B. N., Yin, Z., Caraway, N. P., Katz, R. L., Stass, S. A., and Jiang, F. (2006) Identification of putative oncogenes in lung adenocarcinoma by a comprehensive functional genomic approach. *Oncogene 25*, 2628−2635.
(22) Cao, H., Zhu, Q., Huang, J., Li, B., Zhang, S., Yao, W., and Zhang, Y. (2009) Regulation and functional role of eEF1A2 in pancreatic carcinoma. *Biochem. Biophys. Res. Commun. 380*, 11−16.
(23) Tomlinson, V. A., Newbery, H. J., Bergmann, J. H., Boyd, J., Scott, D., Wray, N. R., Sellar, G. C., Gabra, H., Graham, A., Williams, A. R., and Abbott, C. M. (2007) Expression of eEF1A2 is associated with clear cell histology in ovarian carcinomas: Overexpression of the gene is not dependent on modifications at the EEF1A2 locus. *Br. J. Cancer 96*, 1613−1620.
(24) Novosylna, A. V., Timchenko, A. A., Tiktopulo, E. I., Serdyuk, I. N., Negrutskii, B. S., and El'skaya, A. V. (2007) Characteristics of physical properties of the isoforms of translation elongation factor eEF1A. *Biopolym. Cell 23*, 386−390.
(25) Budkevich, T. V., Timchenko, A. A., Tiktopulo, E. I., Negrutskii, B. S., Shalak, V. F., Petrushenko, Z. M., Aksenov, V. L., Willumeit, R., Kohlbrechner, J., Serdyuk, I. N., and El'skaya, A. V. (2002) Extended conformation of mammalian translation elongation factor 1A in solution. *Biochemistry 41*, 15342−15349.
(26) Kanibolotsky, D. S., Novosyl'na, O. V., Abbott, C. M., Negrutskii, B. S., and El'skaya, A. V. (2008) Multiple molecular dynamics simulation of the isoforms of human translation elongation factor 1A reveals reversible fluctuations between "open" and "closed" conformations and suggests specific for eEF1A1 affinity for Ca^{2+}-calmodulin. *BMC Struct. Biol. 8*, 4.
(27) Soares, D. C., Barlow, P. N., Newbery, H. J., Porteous, D. J., and Abbott, C. M. (2009) Structural models of human eEF1A1 and eEF1A2 reveal two distinct surface clusters of sequence variation and potential differences in phosphorylation. *PLoS One 4* (7), e6315.
(28) Brungraber, E. F. (1962) A simplified procedure for the preparation of "soluble" RNA from rat liver. *Biochem. Biophys. Res. Commun. 8*, 1−3.
(29) Budkevich, T. V., El'skaya, A. V., and Nierhaus, K. H. (2008) Features of 80S mammalian ribosome and its subunits. *Nucleic Acids Res. 36*, 4736−4744.
(30) Amemiya, Y., Ito, K., Yagi, N., Asano, Y., Wakabayashi, K., Ueki, T., and Endo, T. (1995) Large-aperture TV detector with a beryllium-windowed image intensifier for X-ray diffraction. *Rev. Sci. Instrum. 66*, 2290−2294.
(31) Ito, K., Kamikubo, H., Yagi, N., and Amemiya, Y. (2005) Correction method and software for image distortion and nonuniform response in charge-coupled device-based X-ray detectors utilizing X-ray image intensifier. *Jpn. J. Appl. Phys. 44*, 8684−8691.
(32) Svergun, D. I., Barberato, C., and Koch, M. H. C. (1995) CRYSOL: A program to evaluate the X-ray solution scattering of biological macromolecules from atomic coordinates. *J. Appl. Crystallogr. 28*, 768−773.
(33) Schuck, P. (2000) Size-distribution analysis of macromolecules by sedimentation velocity ultracentrifugation and Lamm equation modeling. *Biophys. J. 78*, 1606−1619.
(34) Serdyuk, I. N., Zaccai, N., and Zaccai, J. (2007) *Methods in molecular biophysics. Structure, function, dynamics*, Cambridge University Press, Cambridge, England.
(35) Ortega, A., Amoros, D., and Garcia de la Torre, J. (2011) Prediction of hydrodynamic and other solution properties of rigid proteins from atomic- and residue-level models. *Biophys. J. 101*, 892−898.

(36) Zamyatnin, A. A. (1984) Amino acid, peptide, and protein volume in solution. *Annu. Rev. Biophys. Bioeng. 13*, 145−165.
(37) Chaudhuri, T. K., Das, K. P., and Sinha, N. K. (1993) Surface hydrophobicity of a low molecular weight basic trypsin subtilisin inhibitor from marine turtle eggwhite. *J. Biochem. 113*, 729−733.
(38) Kato, A., and Nakai, S. (1980) Hydrophobicity determined by a fluorescence probe method and its correlation with surface properties of proteins. *Biochim. Biophys. Acta 624*, 13−20.
(39) El'skaya, A. V., and Soldatkin, A. P. (1983) The accuracy of poly(U) translation by different eukaryotic tRNAs. *FEBS Lett. 164*, 93−96.
(40) Silberklang, M., Gillum, A. M., and RajBhandary, U. L. (1979) Use of in vitro ^{32}P labeling in the sequence analysis of nonradioactive tRNAs. *Methods Enzymol. 59*, 58−109.
(41) Morita, K., Bunai, F., and Numata, O. (2008) Roles of three domains of *Tetrahymena* eEF1A in bundling F-actin. *Zool. Sci. 25*, 22−29.
(42) Bunai, F., Ando, K., Ueno, H., and Numata, O. (2006) *Tetrahymena* eukaryotic translation elongation factor 1A (eEF1A) bundles filamentous actin through dimer formation. *J. Biochem. 140*, 393−399.
(43) Lamberti, A., Sanges, C., Chambery, A., Migliaccio, N., Rosso, F., Di Maro, A., Papale, F., Marra, M., Parente, A., Caraglia, M., Abbruzzese, A., and Arcari, P. (2011) Analysis of interaction partners for eukaryotic translation elongation factor 1A M-domain by functional proteomics. *Biochimie 93*, 1738−1746.
(44) Sanges, C., Scheuermann, C., Zahedi, R. P., Sickmann, A., Lamberti, A., Migliaccio, N., Baljuls, A., Marra, M., Zappavigna, S., Reinders, J., Rapp, U., Abbruzzese, A., Caraglia, M., and Arcari, P. (2012) Raf kinases mediate the phosphorylation of eukaryotic translation elongation factor 1A and regulate its stability in eukaryotic cells. *Cell Death Dis.*, e276.
(45) Häsler, J., Rada, C., and Neuberger, M. S. (2012) The cytoplasmic AID complex. *Semin. Immunol. 24* (4), 273−280.
(46) Semisotnov, G. V., Kihara, H., Kotova, N. V., Kimura, K., Amemiya, Y., Wakabayashi, K., Serdyuk, I. N., Timchenko, A. A., Chiba, K., Nikaido, K., Ikura, T., and Kuwajima, K. (1996) Protein globularization during folding. A study by synchrotron small-angle X-ray scattering. *J. Mol. Biol. 262*, 559−574.
(47) Svergun, D. I. (1992) Determination of the regularization parameter in indirect-transform methods using perceptual criteria. *J. Appl. Crystallogr. 25*, 495−503.
(48) Pechmann, S., Levy, E. D., Tartaglia, G. G., and Vendruscolo, M. (2009) Physicochemical principles that regulate the competition between functional and dysfunctional association of proteins. *Proc. Natl. Acad. Sci. U.S.A. 106*, 10159−10164.
(49) Petrushenko, Z. M., Budkevich, T. V., Shalak, V. F., Negrutskii, B. S., and El'skaya, A. V. (2002) Novel complexes of mammalian translation elongation factor eEF1A·GDP with uncharged tRNA and aminoacyl-tRNA synthetase. Implications for tRNA channeling. *Eur. J. Biochem. 269*, 4811−4818.
(50) Petrushenko, Z. M., Negrutskii, B. S., Ladokhin, A. S., Budkevich, T. V., Shalak, V. F., and El'skaya, A. V. (1997) Evidence for the formation of an unusual ternary complex of rabbit liver EF-1α with GDP and deacylated tRNA. *FEBS Lett. 407*, 13−17.
(51) Feigin, L. A., and Svergun, D. I. (1987) *Structure Analysis by Small-Angle X-ray and Neutron Scattering*, Plenum Press, New York.
(52) Negrutskii, B., Vlasenko, D., and El'skaya, A. (2012) From global phosphoproteomics to individual proteins: The case of translation elongation factor eEF1A. *Expert Rev. Proteomics 9* (1), 71−83.
(53) Andersen, G. R., Valente, L., Pedersen, L., Kinzy, T. G., and Nyborg, J. (2001) Structural basis for nucleotide exchange and competition with tRNA in the yeast elongation factor complex eEF1A:eEF1Bα. *Nat. Struct. Biol. 8*, 531−534.
(54) Alexander, P. A., He, Y., Chen, Y., Orban, J., and Bryan, P. N. (2009) A minimal sequence code for switching protein structure and function. *Proc. Natl. Acad. Sci. U.S.A. 106*, 21149−21154.
(55) Alexander, P. A., He, Y., Chen, Y., Orban, J., and Bryan, P. N. (2007) The design and characterization of two proteins with 88% sequence identity but different structure and function. *Proc. Natl. Acad. Sci. U.S.A. 104*, 11963−11968.
(56) Dever, T. E., Costello, C. E., Owens, C. L., Rosenberry, T. L., and Merrick, W. C. (1989) Location of seven post-translational modifications in rabbit elongation factor 1α including dimethyllysine, trimethyllysine, and glycerylphosphorylethanolamine. *J. Biol. Chem. 264*, 20518−20525.
(57) Khan, D. H., He, S., Yu, J., Winter, S., Cao, W., Seiser, C., and Davie, J. R. (2013) Protein kinase CK2 regulates the dimerization of histone deacetylase (HDAC) 1 and HDAC2 during mitosis. *J. Biol. Chem. 288*, 16518−16528.
(58) Ehrenberg, M., Rojas, A. M., Weiser, J., and Kurland, C. G. (1990) How many EF-Tu molecules participate in aminoacyl-tRNA binding and peptide bond formation in *Escherichia coli* translation? *J. Mol. Biol. 211* (4), 739−749.
(59) Khalyfa, A., Carlson, B. M., Dedkov, E. I., and Wang, E. (2003) Changes in protein levels of elongation factors, eEF1A-1 and eEF1A-2/S1, in long-term denervated rat muscle. *Restor. Neurol. Neurosci. 21*, 47−53.
(60) Bosutti, A., Scaggiante, B., Grassi, G., Guarnieri, G., and Biolo, G. (2007) Overexpression of the elongation factor 1A1 relates to muscle proteolysis and proapoptotic p66(ShcA) gene transcription in hypercatabolic trauma patients. *Metabolism 56*, 1629−1634.
(61) Antion, M. D., Hou, L., Wong, H., Hoeffer, C. A., and Klann, E. (2008) mGluR-dependent long-term depression is associated with increased phosphorylation of S6 and synthesis of elongation factor 1A but remains expressed in S6K-deficient mice. *Mol. Cell. Biol. 28*, 2996−3007.
(62) Huang, F., Chotiner, J. K., and Steward, O. (2005) The mRNA for elongation factor 1α is localized in dendrites and translated in response to treatments that induce long-term depression. *J. Neurosci. 25*, 7199−7209.
(63) Hashimoto, K., and Ishima, T. (2011) Neurite outgrowth mediated by translation elongation factor eEF1A1: A target for antiplatelet agent cilostazol. *PLoS One 6* (3), e17431.